Carcinogenesis vol.32 no.7 pp.1093–1099, 2011
doi:10.1093/carcin/bgr079
Advance Access publication May 10, 2011

Evidence of p38γ and p38δ involvement in cell transformation processes

M.Isabel Cerezo-Guisado, Paloma del Reino, Gaëlle Remy, Yvonne Kuma, J.Simon C.Arthur[1], David Gallego-Ortega[2,3] and Ana Cuenda*

Department of Immunology and Oncology, Centro Nacional de Biotecnología/CSIC, Campus de Cantoblanco, 28049 Madrid, Spain, [1]MRC Protein Phosphorylation Unit, Sir James Black Building, School of Life Sciences, University of Dundee, Dundee DD1 5EH, UK and [2]Translational Oncology Unit CSIC/UAM-Hospital La Paz, Centro Nacional de Biotecnología, Campus de Cantoblanco, 28049 Madrid, Spain

[3]Present address: Cancer Research Program, Garvan Institute of Medical Research, Sydney, Australia

*To whom correspondence should be addressed. Tel: +34 915855451; Fax: +34 91 3720493;
Email: acuenda@cnb.csic.esa

The p38 mitogen-activated protein kinase (p38MAPK) signal transduction pathway is an important regulator of cell processes, whose deregulation leads to the development and progression of cancer. Defining the role of each p38MAPK family member in these processes has been difficult. To date, most studies of the p38MAPK pathways focused on function of the p38α isoform, which is widely considered to negatively regulate malignant transformation; nonetheless, few reports address the p38γ and p38δ isoforms. Here, we used embryonic fibroblasts derived from mice lacking p38γ or p38δ and show evidence that these isoforms participate in several processes involved in malignant transformation. We observed that lack of either p38γ or p38δ increased cell migration and metalloproteinase-2 secretion, whereas only p38δ deficiency impaired cell contact inhibition. In addition, lack of p38γ in K-Ras-transformed fibroblasts led to increased cell proliferation as well as tumorigenesis both *in vitro* and *in vivo*. Our results indicate that p38γ and p38δ have a role in the suppression of tumor development.

Introduction

Mitogen-activated protein kinase (MAPK) signaling has a critical role in cell processes whose deregulation leads to cancer development and progression. MAPK pathways link extracellular signals to the machinery that controls fundamental cell activities such as growth, proliferation, differentiation, migration and apoptosis. There are several groups of MAPK in mammalian cells, among which extracellular signal-regulated kinases (ERK), Jun N-terminal kinases (JNK) and p38 kinases are the best characterized (1). The mammalian MAPK p38 subfamily has four members, p38α, p38β, p38γ and p38δ, which share similar protein sequences and are activated by dual phosphorylation mediated by the MAPK kinases MKK3 and MKK6 (2). Based on expression patterns, substrate specificities and sensitivity to chemical inhibitors, p38MAPK can be further divided into two subsets (1,3). One group includes p38α and p38β, which are closely related that might have overlapping functions, whereas p38β appears to be expressed at very low levels, p38α is abundant in most cell types and is the best-described isoform. In contrast, p38γ and p38δ have restricted expression patterns and probably have specialized functions (1,4).

Abbreviations: ERK, extracellular signal-regulated kinase; DMEM, Dulbecco's modified Eagle's medium; JNK, Jun N-terminal kinase; MEF, mouse embryonic fibroblast; MMP, matrix metalloproteinase; MTT, 3-(4,5-dimethylthiazol-2-yl)-2,5-diphenyltetrazolium bromide; PBS, phosphate-buffered saline; RT, room temperature; TPA, 12-O-tetradecanoylphorbol-13-acetate; WT, wild-type.

The p38MAPK subfamily members are included in the group of canonical-signaling pathways involved in the cell transformation process (5–8). Malignant transformation requires deregulation of at least six cell processes, and cancer cells have to acquire the following capabilities: self sufficiency in growth signals, unlimited replication potential, protection against apoptotic cell death, *de novo* angiogenesis and tissue invasion and metastasis (9). p38α negatively regulates cell cycle progression at both the G_1/S and the G_2/M transitions (10,11) and is involved in survival and in the apoptosis induced by many types of cell stress (8). p38α might also directly affect migration, tumor invasion and angiogenesis by inducing expression of some matrix metalloproteinases (MMP) and of the vascular endothelial growth factor A, a potent inducer of tumor survival and angiogenesis (8,12). Subcutaneous xenograft experiments showed that injection of mouse embryonic fibroblasts (MEF) lacking p38α (6,13) or the p38MAPK activators MKK3 and MKK6 (14) caused more oncogene-induced tumors in nude mice than did wild-type (WT) fibroblasts. p38αMAPK pathway function as an *in vivo* tumor suppressor was also shown using genetically modified mice. As p38α knockout impairs placental development and is embryonic lethal, p38α conditional alleles were used to study its implication in cancer development. p38α-deficient mice are sensitive to K-Ras-induced lung carcinogenesis and specific p38α deletion in hepatocytes promotes chemically induced liver cancer (15–17).

Whereas most studies of the p38MAPK pathways to date focused on p38α function in the transformation process, there are few reports on the role of p38γ and p38δ. p38γ is claimed to regulate γ-irradiation-induced G_2 arrest (18); with p38α, it is thought to be an essential component of the pathway that mediates Ras-induced senescence and regulates the tumor-suppressing senescence response in primary human cells (19). In contrast to the numerous reports discussing p38αMAPK function as a tumor suppressor, recent data suggest that p38γ and p38δ might promote tumor development. p38δ was recently shown to mediate 12-*O*-tetradecanoylphorbol-13-acetate (TPA)-induced epidermal cell proliferation in mice, and mice lacking p38δ show reduced susceptibility to the development of TPA-induced skin carcinomas (20). By regulating cell proliferation and invasion, p38δ promotes the malignant phenotype of squamous cell carcinoma (21). p38γ is suggested to be involved in Ras transformation in rat intestinal epithelial cells and in Ras-increased invasion in breast cancer cells (22,23). Most of these studies were performed by overexpressing p38γ or p38δ dominant-negative forms or by p38γ stable transfection of cells. The specific involvement of these two p38 isoforms in transformation has not been analyzed in cells derived from mice lacking p38γ or p38δ. Here, we used p38γ- or p38δ-deficient MEF for the first time to examine their function in several processes involved in malignant transformation. Our results show that both of these p38MAPK regulate cell migration and MMP-2 secretion and that p38δ controls cell contact inhibition. We also show that lack of p38γ in K-Ras-transformed fibroblasts leads to increased cell proliferation and to tumorigenesis. Our results provide evidence of a role for p38γ and p38δ in suppressing tumor development.

Materials and methods

Antibodies

Anti-p38γ and -p38δ antibodies for western blot were generated in sheep against the whole protein and purified as described (3,24). Antibodies to ERK1/ERK2 and phospho-ERK1/ERK2 (Thr202/Tyr204), PKB and phospho-PKB (Ser473), JNK1/2, phospho-p38MAPK (Thr180/Tyr182) and the Myc-Tag antibody were obtained from Cell Signaling Technologies (Hitchin, Hertfordshire, UK). Anti-p38α and -MMP-2 were from Santa Cruz (Santa Cruz, CA), anti-phosphorylated-JNK1/2 (Thr183/Tyr185) from Biosource (Invitrogen, Paisley, UK) and anti-p38β and -α-tubulin from Zymed (San Francisco, CA).

Peroxidase-conjugated rabbit anti-sheep IgG, goat anti-rabbit and rabbit anti-mouse IgG secondary antibodies were from Perbio Science (Northumberland, UK).

Cell culture, stimulation and lysis

Primary fibroblasts were isolated from day 13.5 WT, p38$\gamma^{-/-}$ and p38$\delta^{-/-}$ littermate mouse embryos (25), cultured in Dulbecco's modified Eagle medium with 10% fetal bovine serum, 2 mM L-glutamine, 1% non-essential amino acids, 1% sodium pyruvate, 0.001% 2-mercaptoethanol, 100 U/ml penicillin and 0.1 mg/ml streptomycin [(complete Dulbecco's modified Eagle's medium (DMEM)] and immortalized following the 3T3 protocol (26). Cells were serum starved (16 h) in DMEM supplemented with L-glutamine and antibiotics before stimulation with H_2O_2 (2 mM) or ultraviolet C (200 J/m^2) as indicated in figure legends. Cells were lysed in a solution of 50 mM Tris–HCl pH 7.5, 1 mM ethyleneglycol-bis(aminoethylether)-tetraacetic acid, 1 mM ethylenediaminetetraacetic acid, 0.15 M NaCl, 1 mM sodium orthovanadate, 10 mM NaF, 50 mM sodium β-glycerophosphate, 5 mM pyrophosphate, 0.27 M sucrose, 0.1 mM phenylmethylsulphonyl fluoride, 1% Triton X-100, 0.1% 2-mercaptoethanol and 1 mM benzamidine. Lysates were centrifuged (18 000*g*, 10 min, 4°C), supernatants removed, quick frozen and stored at −80°C. Protein concentration was determined by the Bradford method.

Retroviral infection

To generate retrovirus, 293T cells were transiently transfected with pBabe-Puro-based vector encoding a Myc-tagged K-RasV12 4A (kindly provided by Dr A.Nebreda, CNIO, Madrid, Spain). Retrovirus was collected from culture supernatants at 48 (first supernatant) and 72 h (second supernatant) posttransfection, filtered (0.45 μm polyvinylidene difluoride; Millipore, Bedford, MA) and supplemented with 8 μg/ml polybrene (Sigma, St Louis, MO). MEF (∼5 10^5/10 cm dish) were infected with 5 ml first supernatant, supplemented 24 h later with 3 ml second supernatant and purified 48 h postinfection with 1.5–2.5 μg/ml puromycin.

For the rescue experiments, retroviral infection was performed using a pLHCX vector encoding p38γ kindly provided by Dr Guan Chen, Medical College of Wiscosin, Wiscosin, WI, USA.

Western blot

Protein samples were resolved by sodium dodecyl sulfate–polyacrylamide gel electrophoresis and transferred to nitrocellulose. Membranes were blocked 30 min with 5% non-fat dry milk in 50 mM Tris/HCl (pH 7.5), 0.15 M NaCl and 0.5% Tween (TBS-Tween buffer). Membranes were incubated with 5% non-fat dry milk in TBS-Tween buffer containing 0.5–1 μg/ml of the primary antibody [2 h, room temperature (RT) or overnight at 4°C], washed four times with TBS-Tween buffer and incubated with appropriate secondary antibodies (1 h). Signals were visualized using enhanced chemiluminescence reagent (GE Healthcare, Piscataway, NJ).

Flow cytometry analysis

Cells were trypsinized, resuspended in ice-cold 70% ethanol, fixed (4°C, 30 min) and stored at −20°C. Thawed cells were then resuspended in phosphate-buffered saline (PBS), centrifuged (1000*g*, 4°C, 10 min), resuspended in 1 ml Beckman Coulter DNAprep, incubated (37°C, 30 min) and analyzed on a Cytomics FC500 cytometer (Beckman Coulter, Fullerton, CA).

Immunofluorescence staining

Cells were cultured on 22 mm diameter coverslips, fixed in 4% paraformaldehyde (10 min, RT), blocked in 5% bovine serum albumin in PBS (30 min, RT) and then incubated with primary antibody (2 h, RT) in a humidified chamber. Tubulin was stained using anti-α-tubulin antibody (1:250); secondary antibody was added (1:250, 1 h) and incubated in a dark humidified chamber. DNA was stained with 4′,6-diamidino-2-phenylindole (1 mM, 10 min, RT). Mounting medium was 50% glycerol in PBS. Epifluorescence microscopy was performed using an Olympus FV1000 inverted microscope with PlanApo x63 1.4 NA oil immersion objectives. Images were assembled using Adobe Photoshop.

Wound closure assay

Cells were plated in culture dishes at confluence and pretreated with mitomycin C (25 μg/ml, 1 h) before the injury line was made with a pipette tip (∼0.5 mm diameter). After rinsing with PBS, cells were allowed to migrate in complete DMEM and photographed (×4) at the indicated times.

Zymography

To determine MMP-2 activity levels, 5 × 10^4 cells were plated in 24-well dishes. Culture medium was replaced with 0.5 ml fresh serum-free medium and incubated (16 h). Medium was then collected, mixed with an equal volume of non-reducing Laemmli sample buffer and applied to 8% sodium dodecyl sulfate–polyacrylamide gel electrophoresis gels polymerized in the presence of 0.04% gelatin. After electrophoresis, gels were washed with 2.5% Triton X-100 (30 min) to remove sodium dodecyl sulfate, rinsed once with substrate buffer (50 mM Tris–HCl, pH 8, 1 mM $CaCl_2$, 0.02% NaN_3) and incubated (37°C, overnight) in substrate buffer to allow protein renaturation and MMP activation. The position of the MMP was visualized by Coomassie Brilliant Blue R-250 staining (Bio-Rad, Hercules, CA).

Proliferation assays

Cell proliferation assays were performed using the 3-(4,5-dimethylthiazol-2-yl)-2,5-diphenyltetrazolium bromide (MTT) cell proliferation Kit I (Roche Diagnostics, Mannheim, Germany). Cells (1 to 5 × 10^3 cells per well) were seeded in triplicate, and cell numbers were monitored over the times indicated in the figures.

Focus formation assays

Approximately 7.5 × 10^5 cells were plated per 6 cm dish. Culture medium was changed every 3–4 days. After 21 days, foci were fixed and stained with 0.1% crystal violet (Sigma).

Soft agar assay

To measure anchorage-independent growth in soft agar, cells were cultured in 6 cm plates containing two agar layers. The bottom layer consisted of complete DMEM with 20 mM *N*-2-hydroxyethylpiperazine-*N*′-2-ethanesulfonic acid and 0.5% agar, and the top layer contained 1 × 10^5 cells embedded in complete DMEM with 20 mM *N*-2-hydroxyethylpiperazine-*N*′-2-ethanesulfonic acid and 0.35% agar. Complete DMEM was added to the top layer every 3 days to prevent drying of the gel. After 3–4 weeks, colonies were stained with 0.1% crystal violet.

In vivo tumorigenicity assay

For tumorigenicity assays in nude mice (*nu/nu*), cells were resuspended in DMEM just before inoculation (10^6 MEF/0.1 ml/mouse flank) and injected subcutaneously into immunosuppressed female *nu/nu* mice (Charles River Laboratories, Wilmington, MA). Tumor growth was monitored weekly for ∼4 weeks. Tumor volume was calculated by the formula: $V = (D \times d^2)/2$, where D and d are the longest and shortest diameter in millimeters, respectively.

Results

Lack of p38γ affects activation of p38α but not of other MAPK

To study the role of p38γ and p38δ in cell transformation, embryonic fibroblasts from WT and p38γ (p38$\gamma^{-/-}$) or p38δ (p38$\delta^{-/-}$)-null mice were immortalized using the 3T3 protocol (see Methods). p38γ protein and messenger RNA are expressed in WT and in p38$\delta^{-/-}$ MEF but are not detectable in p38$\gamma^{-/-}$ MEF, whereas p38δ protein and messenger RNA are not expressed in p38$\delta^{-/-}$ MEF but are found in WT and p38$\gamma^{-/-}$ MEF (Figure 1A and Supplementary Table I is available at *Carcinogenesis* Online). p38α and p38β levels were similar in WT and knockout MEF, showing that deletion of p38γ or p38δ did not affect p38α and p38β expression (Figure 1A and Supplementary Table I is available at *Carcinogenesis* Online). We examined the effect of p38γ and p38δ deficiency on the activation of several kinase pathways in response to oxidative stress, a potent activator of MAPK pathways. We induced stress in MEF by exposure to H_2O_2, then analyzed phosphorylation of p38α, ERK1/2, JNK1/2 and PKB and observed similar activation of these kinases in WT and p38$\delta^{-/-}$ MEF. Basal p38α activity was much higher in p38$\gamma^{-/-}$ cells than in WT controls and was further stimulated by H_2O_2 (Figure 1A). Basal JNK1/2 phosphorylation was also observed in p38$\gamma^{-/-}$ cells compare to WT control (Figure 1A). The same result was observed in a different pool of p38$\gamma^{-/-}$ and WT MEF, which rule out any effects associated with a particular cell preparation (Supplementary Figure 1 is available at *Carcinogenesis* Online). To determine whether the increase in p38α activity was also time and/or stimulus dependent, we exposed WT and p38$\gamma^{-/-}$ MEF to H_2O_2 or ultraviolet C irradiation for distinct periods and analyzed p38α phosphorylation. The transient p38α activation induced by both stimuli was again stronger in p38$\gamma^{-/-}$ than in WT MEF (Figure 1B). These results suggest that p38γ modulates the intensity of p38α pathway activation and that neither p38γ nor p38δ regulate the activation of these pathways in oxidative stress conditions.

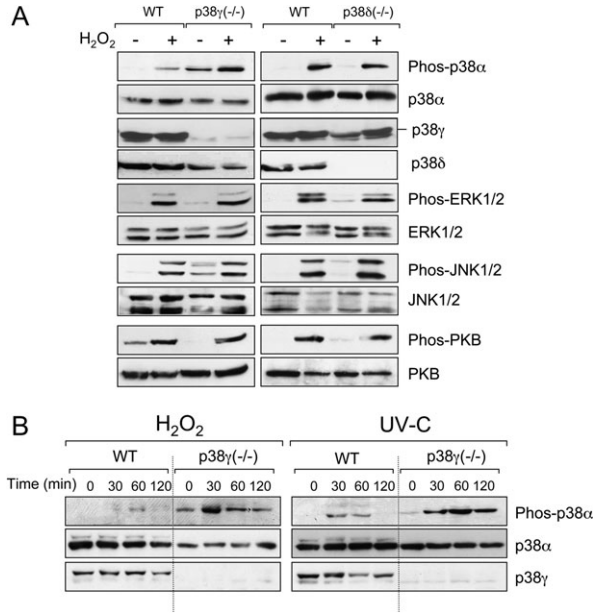

Fig. 1. Activation of kinase pathways in p38γ- and p38δ-deficient cells. (**A**) WT, p38$\gamma^{-/-}$and p38$\delta^{-/-}$ MEF were exposed to 2 mM H_2O_2 (1 h). Cell lysates (50 μg) were immunoblotted with antibodies to active phosphorylated-p38α (Phos-p38α), active phosphorylated-ERK1/2 (Phos-ERK1/2), active phosphorylated-JNK1/2 (Phos-JNK1/2) or active phosphorylated-PKB (Phos-PKB). Total protein levels of p38α, p38γ, p38δ, ERK1/2, JNK1/2 and PKB were measured in the same lysates and used as loading controls. Representative blots are shown. Similar results were obtained in at least two independent experiments. (**B**) WT and p38$\gamma^{-/-}$ fibroblasts were exposed to 2 mM H_2O_2 for the times indicated or to ultraviolet C irradiation (200 J/m^2) followed by incubation (37°C) as indicated. p38α activation was examined as in (A). Total protein level of p38γ was measured in the same lysates, and total p38α was used as loading control. Results were similar in at least two independent experiments.

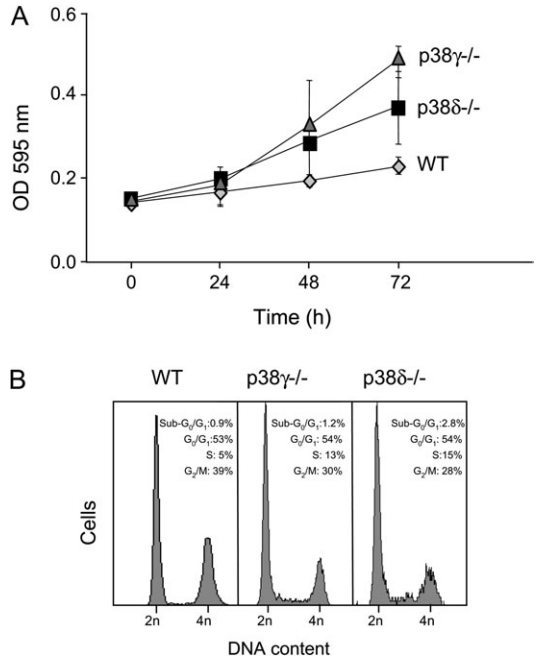

Fig. 2. Effect of p38γ and p38δ on proliferation and cell cycle progression. (**A**) Cell proliferation in WT (grey diamond), p38$\gamma^{-/-}$ (grey triangle) and p38$\delta^{-/-}$ (black square) fibroblasts was determined using MTT (see Methods). Cells (1×10^3) were seeded in triplicate, and cell numbers monitored over the course of 3 days. Values shown are mean ± standard deviation for three independent experiments. (**B**) Subconfluent WT, p38$\gamma^{-/-}$ and p38$\delta^{-/-}$ fibroblasts were collected and DNA content analyzed by flow cytometry. Cell cycle profiles are representative of three independent experiments. The percentage of cells in each cell cycle phase was calculated using CytomicsRXP Analysis software. The percentage of total cells in sub-G_0/G_1 (apoptotic cells), G_0/G_1, S and G_2/M phase are shown.

Proliferation of p38γ- and p38δ-deficient fibroblasts

p38MAPK pathway components such as p38α, MKK3, MKK6 or the phosphatase Wip-1 are implicated in proliferation and cell cycle progression in several culture systems (5,8,14,27). To determine whether p38γ and/or p38δ also affect proliferation, we measured cell culture growth for 3 days in medium supplemented with 10% fetal bovine serum; we found no notable differences between p38$\gamma^{-/-}$ and p38$\delta^{-/-}$ MEF, although they proliferated slightly more rapidly than WT fibroblasts (Figure 2A). Similar percentages of total cells were found in each cell cycle phase for subconfluent WT, p38$\gamma^{-/-}$ and p38$\delta^{-/-}$ MEF cultures (Figure 2B). These data suggest that both p38γ and p38δ control MEF proliferation without affecting cell cycle progression. We nonetheless cannot rule out increased function by another p38MAPK protein to compensate for loss of p38γ or p38δ.

p38γ and p38δ regulate cell migration

To characterize p38γ and p38δ effects on fibroblast morphology, we analyzed all three MEF types by phase contrast microscopy. WT, p38$\gamma^{-/-}$ and p38$\delta^{-/-}$ cells were similar in subconfluent cultures, showing the characteristic flattened appearance of embryonic fibroblasts (Figure 3A). Immunofluorescence microscopy using a monoclonal anti-α-tubulin antibody showed similar microtubule networks in WT and p38$\delta^{-/-}$ MEF (Figure 3A), whereas tubulin localized at one side of the nucleus in p38$\gamma^{-/-}$ MEF. This result indicates that lack of p38γ affects tubulin organization in fibroblasts, probably through regulation of cytoskeletal protein complexes (28).

Since we observed differences in microtubule networks in p38$\gamma^{-/-}$ compared with p38$\delta^{-/-}$ and WT MEF, we studied the effect on cell migration of p38γ or p38δ deficiency compared with WT (Figure 3B and C). In a scratch assay using cells treated with mitomycin C to block proliferation, the rate of wound healing showed that p38$\gamma^{-/-}$ and p38$\delta^{-/-}$ cells migrate more rapidly than WT MEF. The average time of wound healing closure was 14.5 ± 2 h in p38$\gamma^{-/-}$, 19.0 ± 4.0 h in p38$\delta^{-/-}$ and 30.5 ± 7.0 h in WT cells. As enhanced cell migration is often accompanied by MMP secretion (29), we compared MMP-2 protein expression in p38$\gamma^{-/-}$, p38$\delta^{-/-}$ and WT MEF. MMP-2 (∼72 kDa type IV collagenase, gelatinase A) is one of the main MMP produced by fibroblasts *in vitro* (30). Immunoblot showed that protein levels were similar in WT, p38$\gamma^{-/-}$ and p38$\delta^{-/-}$ MEF (Figure 3D). Semiquantitative zymography of MMP-2 enzyme activity showed that both p38γ- and p38δ-null MEF secreted more pro-MMP-2 and MMP-2 than WT cells; MMP-9 (∼92 kDa type IV collagenase, gelatinase B) secretion was also observed in p38$\delta^{-/-}$ cells (Figure 3E). Our data indicate that both p38γ and p38δ regulate cell migration and MMP-2 secretion without affecting its production.

p38δ deficiency affects contact inhibition in fibroblasts

As impaired contact inhibition is considered a hallmark of cell transformation (Hanahan and Weinberg 2000), and p38α is crucial for this process (31,32), we tested whether p38γ and/or p38δ were necessary for contact inhibition. Using phase contrast microscopy, we compared the culture saturation density of immortalized p38$\gamma^{-/-}$and p38$\delta^{-/-}$ with WT MEF. p38$\delta^{-/-}$ fibroblast morphology changed after reaching confluence; in normal growth conditions, these cells became more elongated, stopped growing as monolayers and spontaneously formed foci (Figure 4A); there were no apparent differences in saturation density between WT and p38$\gamma^{-/-}$ MEF. We observed multilayered focus formation in confluent p38$\delta^{-/-}$ but not in p38$\gamma^{-/-}$ or WT cells (Figure 4B), indicating absence of contact inhibition in p38$\delta^{-/-}$ fibroblasts. To confirm a role for p38δ in contact inhibition, we cultured p38$\delta^{-/-}$ and WT MEF beyond 100%

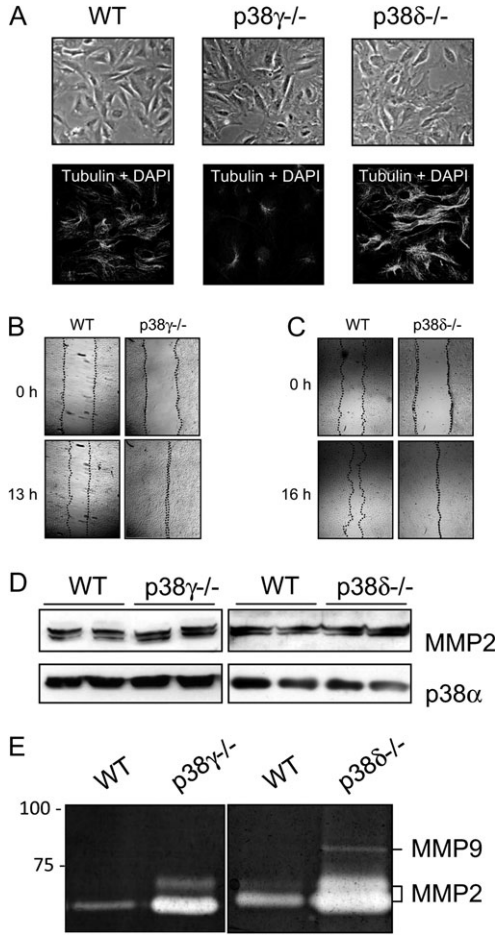

Fig. 3. p38γ and p38δ regulate cell migration and MMP-2 secretion. (**A**) Morphology of WT, p38$\gamma^{-/-}$ and p38$\delta^{-/-}$ fibroblasts was examined by phase contrast microscopy (top). Microtubules (green) were examined by fluorescence microscopy after staining cells with α-tubulin antibody; nuclei are 4′,6-diamidino-2-phenylindole stained (blue) (bottom). WT and p38$\gamma^{-/-}$ (**B**) or p38$\delta^{/}$ (**C**) fibroblasts were plated to confluence, the monolayer scratched and cells allowed to migrate for 13 or 16 h, respectively. Similar results were obtained in 12 independent experiments. (**D**) Lysates (50 μg) from WT, p38$\gamma^{-/-}$ and p38$\delta^{-/-}$ fibroblasts were immunoblotted with anti-MMP-2 antibody. Total protein levels of p38αMAPK were measured in the same lysates and used as loading controls. (**E**) Supernatants were collected from WT, p38$\gamma^{-/-}$ and p38$\delta^{-/-}$ cultures and MMP activity determined by gelatin zymography (see Methods). Areas of gelatinase (MMP) activity were detected as clear bands on the blue-stained gelatin background. Results were similar in at least two independent experiments.

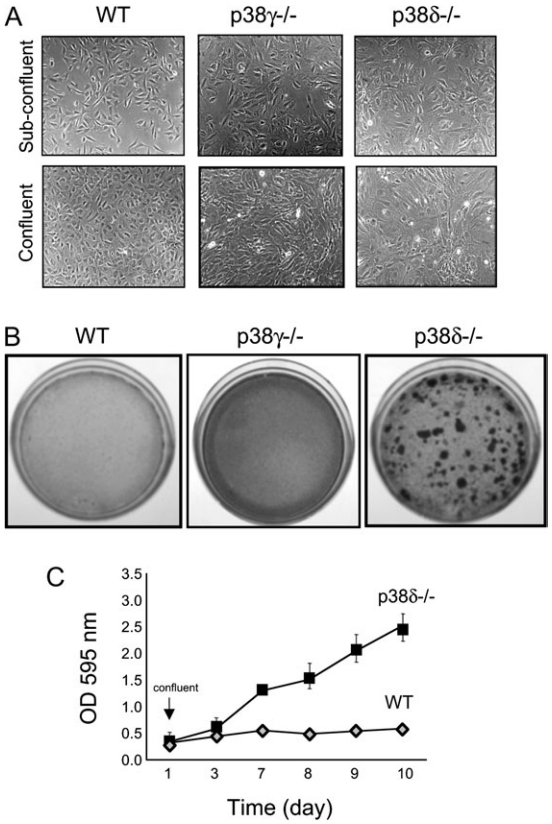

Fig. 4. p38δ deficiency abolishes cell contact inhibition. (**A**) Representative fields showing the morphology of subconfluent fibroblast cultures (top) and saturation density of WT, p38$\gamma^{-/-}$ and p38$\delta^{-/-}$ fibroblasts 2 days after confluence was reached (bottom). (**B**) WT, p38$\gamma^{-/-}$ and p38$\delta^{-/-}$ fibroblasts were analyzed for focus formation over the course of 3 weeks. (**C**) Proliferation of WT (grey diamond) and p38$\delta^{-/-}$ (black square) fibroblasts was determined using MTT. Cells (5×10^3) were seeded in triplicate, and cell numbers monitored over the course of 10 days. Values shown are mean ± standard deviation for two independent experiments. Black arrow indicates the time at which the culture reached confluence.

confluence and determined whether cells continued to grow. Cells were plated and cultured for 10 days, with medium changes every 2–3 days. Both lines had a similar initial growth rate; when cells reached confluence, WT fibroblasts ceased proliferating, whereas the p38$\delta^{-/-}$ culture continued to grow and showed an almost 5-fold higher saturation density than WT fibroblasts (Figure 4C).

p38γ has a role in K-Ras transformation

Evidence suggests that p38γ participates in Ras-induced cell transformation (22,23,33). These studies were based on overexpression of p38γ dominant-negative forms or by p38γ stable transfection; nonetheless, experiments using p38$\gamma^{-/-}$ cells have not been reported. We therefore studied the effect of p38γ on K-Ras-induced transformation using p38γ-null cells. Fibroblasts from p38$\gamma^{-/-}$ or WT (p38$\gamma^{+/+}$) mouse embryos were immortalized and retrovirus infected to stably express K-RasV12. p38γ and K-Ras expression in these cells were visualized in western blot (Figure 5A). Comparison of growth of p38$\gamma^{-/-}$ MEF and p38$\gamma^{+/+}$ MEF-expressing K-RasV12 showed that K-RasV12-p38$\gamma^{-/-}$ cells proliferate substantially faster than K-RasV12-p38$\gamma^{+/+}$ MEF (Figure 5B). In a soft agar cell transformation assay, we compared anchorage-independent colony formation of K-RasV12-p38$\gamma^{-/-}$ and K-RasV12-p38$\gamma^{+/+}$ MEF. K-RasV12-transformed p38$\gamma^{-/-}$ MEF, which formed more and larger foci than WT MEF (Figure 5C). The ability of p38γ-null cells to grow in soft agar, considered a better marker for *in vitro* tumorigenesis than proliferation rate, suggested greater malignant transformation potential of these cells.

Lack of p38γ increases the in vivo tumorigenic properties of K-Ras-transformed MEF

To examine the *in vivo* relevance of our observations, p38$\gamma^{-/-}$ or p38$\gamma^{+/+}$ immortalized MEF-expressing K-RasV12 was injected into athymic nude mice and tumor formation examined. K-RasV12-p38$\gamma^{+/+}$ MEF formed no tumors, whereas K-RasV12/p38$\gamma^{-/-}$ MEF formed large rapidly growing tumors in all mice (Figure 6A). Over a 4 week period, all 12 mice injected with K-RasV12-p38$\gamma^{-/-}$ cells developed tumors, which first appeared at the injection site at day 16 (Figure 6A). To address the Ras requirement in this process, we tested tumorigenicity of p38$\gamma^{-/-}$ or WT MEF; these cells did not form tumors (data not shown). Loss of p38γ in K-Ras-transformed MEF, thus appears sufficient to confer tumorigenesis *in vivo*.

We also performed rescued experiments in which p38γ expression in K-RasV12/p38$\gamma^{-/-}$ cells was restored (Figure 6B). Remarkably,

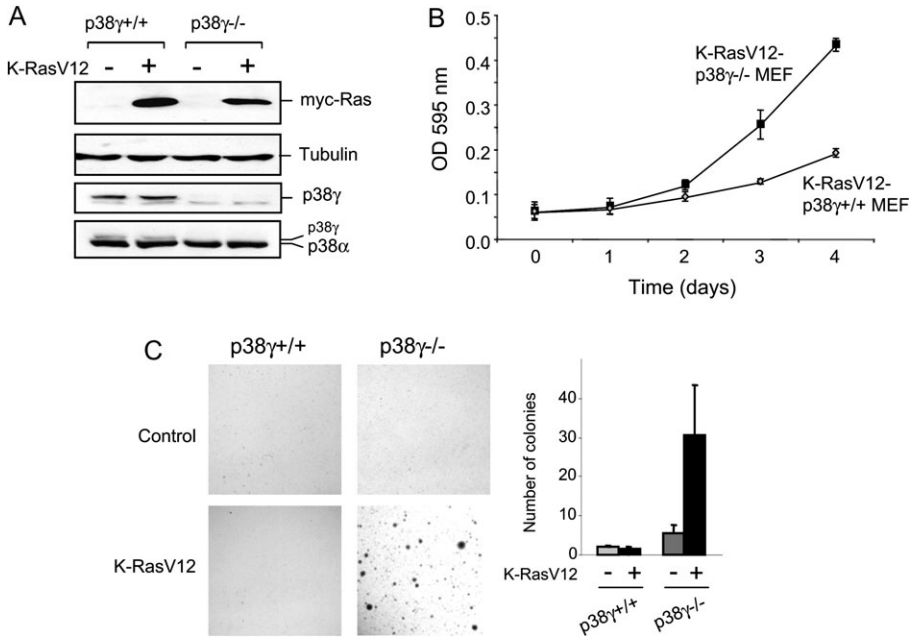

Fig. 5. p38γ regulates K-RasV12-induced malignant transformation. (**A**) Cell extracts (50 μg) from WT ($p38\gamma^{+/+}$) and $p38\gamma^{-/-}$ fibroblasts that did or did not express K-RasV12 were examined by immunoblotting with the indicated antibodies. (**B**) Proliferation of $p38\gamma^{+/+}$ or $p38\gamma^{-/-}$ fibroblasts-expressing K-RasV12 was determined over the course of 4 days. Values shown are mean ± standard deviation for two experiments. (**C**) Analysis of anchorage-independent growth in soft agar of $p38\gamma^{+/+}$ and $p38\gamma^{-/-}$ fibroblasts that did or did not express K-RasV12. Representative micrographs show the appearance of colonies (left); average colony number (right). Values are mean ± standard deviation for triplicates from two experiments.

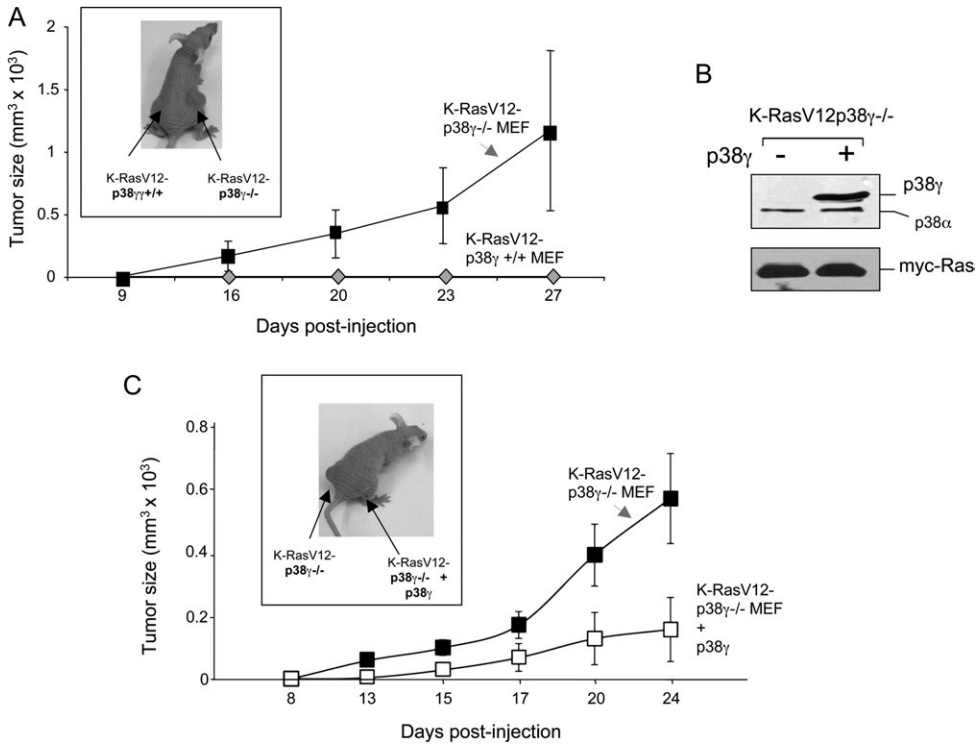

Fig. 6. p38γ deletion increases tumorigenesis of K-Ras-transformed cells. (**A**) Immunodeficient nude mice were injected subcutaneously with $p38\gamma^{+/+}$ and $p38\gamma^{-/-}$ fibroblasts-expressing K-RasV12, and tumor volume was measured periodically as indicated. Values shown are mean ± standard deviation for 12 mice. Inset: Representative photograph of mouse tumor at day 23 is illustrated. Arrows indicate injection sites and tumor location. (**B**) Cell extracts (50 μg) from K-RasV12-$p38\gamma^{-/-}$ fibroblasts that did or did not express p38γ were examined by immunoblotting with the indicated antibodies. (**C**) Immunodeficient nude mice were injected subcutaneously with K-RasV12-$p38\gamma^{-/-}$ and K-RasV12-$p38\gamma^{-/-}$-expressing p38γ fibroblasts, and tumor volume was measured periodically as indicated. Values shown are mean ± standard deviation for six mice. Inset: Representative photograph of mouse tumor at day 24 is illustrated. Arrows indicate injection sites and tumor location.

the differences between K-RasV12-p38$\gamma^{+/+}$ and K-RasV12/p38$\gamma^{-/-}$ cells in tumor formation were largely rescued by the reintroduction of p38γ (Figure 6C). The tumors formed by K-RasV12-p38$\gamma^{+/+}$ + p38γ MEF appeared few days latter and were >70% smaller than those formed by K-RasV12/p38$\gamma^{-/-}$ MEF (Figure 6C). These results indicate that the differences observed in Figure 6A are mostly due to the lack of p38γ and not to secondary genetic alterations.

Discussion

There have been many recent studies of p38αMAPK in cancer, showing that inactivation of this pathway enhances cell transformation *in vitro* and promotes cancer development in mouse models (reviewed in ref. 8). In comparison, the functions of p38γ and p38δ in cell transformation are largely uncharacterized. Here, we used immortalized p38$\gamma^{-/-}$ and p38$\delta^{-/-}$ MEF to study their participation in transformation processes and provide several lines of evidence indicating that p38γ and p38δ act as tumor suppressors.

Contact inhibition is the process by which cells cease to proliferate when they reach confluence, despite availability of extracellular nutrients and growth factors. Deregulation of contact inhibition is a hallmark of malignant cell transformation, as it leads to hyperplasia *in vivo* and facilitates tumor progression. Although the mechanism of regulation by contact inhibition is not fully known, evidence implicates p38α in this process (31,32). p38α induces degradation of the epidermal growth factor receptor through downregulation of the epidermal growth factor receptor-stabilizing protein Sprouty2. p38α-deficient cells thus show accumulation and sustained activation of epidermal growth factor receptor; this impairs $p27^{Kip1}$ accumulation and cell cycle arrest and causes cell overgrowth and oncogenic transformation (32). To analyze the role of p38γ and p38δ in contact inhibition, we compared growth curves of immortalized WT, p38$\gamma^{-/-}$ and p38$\delta^{-/-}$ fibroblasts. p38γ- and p38δ-deficient MEF had a slightly more rapid growth rate than WT cells, similar to results for cells lacking the upstream p38MAPK activators MKK3 and MKK6 (14). p38$\delta^{-/-}$ cells formed spontaneous foci and showed ∼5-fold higher saturation density than WT cells, indicating impaired contact inhibition. Foci formation is usually an indication for transformation; however, injection of p38$\delta^{-/-}$ cells into nude mice did not lead to tumor formation (data not shown). In contrast to our findings, it has been suggested an *in vivo* role for p38δ in promoting cell proliferation and tumor development in epidermis since p38δ-null mice are more resistant to 7,12-dimethylbenz[a]anthracene-TPA-induced skin papillomas (20). This discrepancy in the results could be due not only to the difference in the experimental model used in the two studies but also to the type of cell(s) and process(es) that is/are involved in each experimental approach. Opposing roles in tumor development has also been reported for the isoform p38α (1).

Nonetheless, our results suggest that p38δ is an important component in the control of cell density and cell contact inhibition. Although we have found that p38γ deficiency does not affect these processes, we cannot rule out a role for this isoform. Since we report that p38α activity, necessary for cell–cell contact inhibition, is enhanced in p38γ-deficient cells, p38α might compensate for the lack of p38γ.

One of the hallmarks of cancer cells is the ability to leave their primary site of growth and move into different tissue compartments. Here, we also established that both p38γ and p38δ control cell migration. At difference from findings for p38α (12,34), the lack of either p38γ or p38δ led to increased cell mobility accompanied by greater secretion and activation of MMP-2, with no change in expression. Several studies show a correlation between MMP-2 and/or MMP-9 levels and an increase in cancer cell motility and invasiveness (29). However, we found that the treatment of p38$\gamma^{-/-}$ and p38$\delta^{-/-}$ MEF with the general MMP inhibitor 2R-[(4-biphenylsulfonyl)amino]-*N*-hydroxy-3-phenylpropinamide (BiPS) did not block the increase in cell migration (data not shown), indicating that MMP-2 does not mediate the enhanced mobility in p38$\gamma^{-/-}$ and p38$\delta^{-/-}$ cells. Our findings show therefore that lack of p38γ or p38δ causes increased cell mobility and that the increase in MMP-2 activation has a yet unidentified function.

Numerous reports indicate that the p38MAPK pathway controls Ras oncogene activity by suppressing it (reviewed in ref. 35). p38α activation leads either to inhibition of Ras-dependent growth or to induction of Ras-dependent death (35). These observations were consolidated by experiments showing increased Ras-induced tumorigenesis through knockout of the p38-activating kinases MKK3 and MKK6 (14) or of p38α (6). Here, we show that in K-Ras-transformed fibroblasts, p38γ deletion leads to increased cell proliferation, anchorage-independent colony formation and tumorigenesis. These results contrast with reports suggesting that p38γ enhances Ras transformation in rat intestinal epithelial cells and Ras-increased invasion in breast cancer cells (22,23). As our study was restricted to MEF, the divergent findings could reflect cell type-based differences in the role of p38γ in Ras transformation. Depending on cell context, K-Ras increases or decreases intracellular reactive oxygen species levels, which activate p38MAPK (36,37). In addition, factors involved in Ras-mediated cell responses differ between fibroblasts and epithelial cells (38); for example, K-Ras induces p38γ protein expression in rat intestinal epithelial IEC-6 cells but not in mouse NIH3T3 fibroblasts (23).

In summary, we report that in mouse fibroblasts, p38δ regulates cell–cell contact inhibition and both p38γ and p38δ control cell migration. Moreover, in K-Ras-transformed fibroblasts, lack of p38γ enhances cell proliferation and tumorigenesis both *in vitro* and *in vivo*. Our results reveal previously unreported roles for p38γ and p38δ in cells transformation processes and provide evidence that these p38 isoforms act as tumor suppressors and might protect cells against oncogene-induced transformation.

Supplementary material

Supplementary Table 1 and Figure 1 can be found at http://carcin.oxfordjournals.org/

Funding

Spanish Ministry for Science and Innovation (MICINN; BFU2007-67577; BFU2010-19734 to A.C.). M.I.C. is a recipient of the FIS Sara Borrell award from the Instituto de Salud Carlos III.

Acknowledgements

We thank Drs A.Nebreda, I.Dolado, J.C.Lacal, M.J.Lorenzo, F.Centeno and A.Álvarez-Barrientos for reagents and helpful advice, L.Almonacid for help with the real-time polymerase chain reaction, A.Checa for microscopy and C.Mark for editorial assistance.

Conflict of Interest Statement: None declared.

References

1. Cuenda,A. *et al*. (2007) p38 MAP-kinases pathway regulation, function and role in human diseases. *Biochim. Biophys. Acta*, **1773**, 1358–1375.
2. Remy,G. *et al*. (2010) Differential activation of p38MAPK isoforms by MKK6 and MKK3. *Cell Signal.*, **22**, 660–667.
3. Cuenda,A. *et al*. (1997) Activation of stress-activated protein kinase-3 (SAPK3) by cytokines and cellular stresses is mediated via SAPKK3 (MKK6); comparison of the specificities of SAPK3 and SAPK2 (RK/p38). *EMBO J.*, **16**, 295–305.
4. Iñesta-Vaquera,F. *et al*. (2008) Alternative p38MAPK pathways. Stress Activated Protein Kinases. *Topics in Current Genetics*. **Vol. 20**, Springer-Verlag, Heidelberg, Germany, pp. 17–26.
5. Bulavin,D.V. *et al*. (2004) p38 MAP kinase's emerging role as a tumor suppressor. *Adv. Cancer Res.*, **92**, 95–118.
6. Dolado,I. *et al*. (2007) p38alpha MAP kinase as a sensor of reactive oxygen species in tumorigenesis. *Cancer Cell*, **11**, 191–205.
7. Han,J. *et al*. (2007) The pathways to tumor suppression via route p38. *Trends Biochem. Sci.*, **32**, 364–371.
8. Wagner,E.F. *et al*. (2009) Signal integration by JNK and p38 MAPK pathways in cancer development. *Nat. Rev. Cancer*, **9**, 537–549.
9. Hanahan,D. *et al*. (2000) The hallmarks of cancer. *Cell*, **100**, 57–70.

10. Ambrosino,C. *et al*. (2001) Cell cycle regulation by p38 MAP kinases. *Biol. Cell*, **93**, 47–51.
11. Thornton,T.M. *et al*. (2009) Non-classical p38 map kinase functions: cell cycle checkpoints and survival. *Int. J. Biol. Sci.*, **5**, 44–51.
12. Rousseau,S. *et al*. (2006) CXCL12 and C5a trigger cell migration via a PAK1/2-p38alpha MAPK-MAPKAP-K2-HSP27 pathway. *Cell Signal.*, **18**, 1897–1905.
13. Bulavin,D.V. *et al*. (2002) p38 and Chk1 kinases: different conductors for the G(2)/M checkpoint symphony. *Curr. Opin. Genet. Dev.*, **12**, 92–97.
14. Brancho,D. *et al*. (2003) Mechanism of p38 MAP kinase activation in vivo. *Genes. Dev.*, **17**, 1969–1978.
15. Hui,L. *et al*. (2007) p38alpha: a suppressor of cell proliferation and tumorigenesis. *Cell Cycle*, **6**, 2429–2433.
16. Sakurai,T. *et al*. (2008) Hepatocyte necrosis induced by oxidative stress and IL-1 alpha release mediate carcinogen-induced compensatory proliferation and liver tumorigenesis. *Cancer Cell*, **14**, 156–165.
17. Ventura,J.J. *et al*. (2007) p38alpha MAP kinase is essential in lung stem and progenitor cell proliferation and differentiation. *Nat. Genet.*, **39**, 750–758.
18. Wang,X. *et al*. (2000) Involvement of the MKK6-p38gamma cascade in gamma-radiation-induced cell cycle arrest. *Mol. Cell. Biol.*, **20**, 4543–4552.
19. Kwong,J. *et al*. (2009) p38alpha and p38gamma mediate oncogenic ras-induced senescence through differential mechanisms. *J. Biol. Chem.*, **284**, 11237–11246.
20. Schindler,E.M. *et al*. (2009) p38delta Mitogen-activated protein kinase is essential for skin tumor development in mice. *Cancer Res.*, **69**, 4648–4655.
21. Junttila,M.R. *et al*. (2007) p38alpha and p38delta mitogen-activated protein kinase isoforms regulate invasion and growth of head and neck squamous carcinoma cells. *Oncogene*, **26**, 5267–5279.
22. Qi,X. *et al*. (2006) p38gamma mitogen-activated protein kinase integrates signaling crosstalk between Ras and estrogen receptor to increase breast cancer invasion. *Cancer Res.*, **66**, 7540–7547.
23. Tang,J. *et al*. (2005) Essential role of p38gamma in K-Ras transformation independent of phosphorylation. *J. Biol. Chem.*, **280**, 23910–23917.
24. Goedert,M. *et al*. (1997) Activation of the novel stress-activated protein kinase SAPK4 by cytokines and cellular stresses is mediated by SKK3 (MKK6); comparison of its substrate specificity with that of other SAP kinases. *EMBO J.*, **16**, 3563–3571.
25. Wiggin,G.R. *et al*. (2002) MSK1 and MSK2 are required for the mitogen- and stress-induced phosphorylation of CREB and ATF1 in fibroblasts. *Mol. Cell. Biol.*, **22**, 2871–2881.
26. Todaro,G.J. *et al*. (1963) Quantitative studies of the growth of mouse embryo cells in culture and their development into established lines. *J. Cell Biol.*, **17**, 299–313.
27. Takekawa,M. *et al*. (2000) p53-inducible wip1 phosphatase mediates a negative feedback regulation of p.38 MAPK-p53 signaling in response to UV radiation. *EMBO J.*, **19**, 6517–6526.
28. Sabio,G. *et al*. (2005) p38gamma regulates the localisation of SAP97 in the cytoskeleton by modulating its interaction with GKAP. *EMBO J.*, **24**, 1134–1145.
29. Sternlicht,M.D. *et al*. (2001) How matrix metalloproteinases regulate cell behavior. *Annu. Rev. Cell Dev. Biol.*, **17**, 463–516.
30. Droppelmann,C.A. *et al*. (2009) Matrix metalloproteinase-2-deficient fibroblasts exhibit an alteration in the fibrotic response to connective tissue growth factor/CCN2 because of an increase in the levels of endogenous fibronectin. *J. Biol. Chem.*, **284**, 13551–13561.
31. Faust,D. *et al*. (2005) p38alpha MAPK is required for contact inhibition. *Oncogene*, **24**, 7941–7945.
32. Swat,A. *et al*. (2009) Cell density-dependent inhibition of epidermal growth factor receptor signaling by p38alpha mitogen-activated protein kinase via Sprouty2 downregulation. *Mol. Cell. Biol.*, **29**, 3332–3343.
33. Qi,X. *et al*. (2007) p38alpha antagonizes p38gamma activity through c-Jun-dependent ubiquitin-proteasome pathways in regulating Ras transformation and stress response. *J. Biol. Chem.*, **282**, 31398–31408.
34. Kim,M.S. *et al*. (2003) p38 kinase is a key signaling molecule for H-Ras-induced cell motility and invasive phenotype in human breast epithelial cells. *Cancer Res.*, **63**, 5454–5461.
35. Loesch,M. *et al*. (2008) The p38 MAPK stress pathway as a tumor suppressor or more? *Front. Biosci.*, **13**, 3581–3593.
36. Maciag,A. *et al*. (2005) Reactive oxygen species and lung tumorigenesis by mutant K-ras: a working hypothesis. *Exp. Lung Res.*, **31**, 83–104.
37. Santillo,M. *et al*. (2001) Opposing functions of Ki- and Ha-Ras genes in the regulation of redox signals. *Curr. Biol.*, **11**, 614–619.
38. Moon,A. *et al*. (2000) H-ras, but not N-ras, induces an invasive phenotype in human breast epithelial cells: a role for MMP-2 in the H-ras-induced invasive phenotype. *Int. J. Cancer*, **85**, 176–181.

Received December 9, 2010; revised March 30, 2011; accepted April 22, 2011